Flux Penetration and Overcritical Currents in Flat Superconductors with Irradiation-Enhanced Edge Pinning: Theory and Experiment

Th. Schuster, M. V. Indenbom,* H. Kuhn, and E. H. Brandt
Max-Planck-Institut für Metallforschung, Institut für Physik, D-70506 Stuttgart, Germany

M. Konczykowski
Laboratoire des Solides Irradiés, Ecole Polytechnique, 91128 Palaiseau, France
(Received 14 March 1994)

Penetration of perpendicular magnetic flux into a $Bi_2Sr_2CaCu_2O_{8+\delta}$ single crystal platelet with irradiation-enhanced pinning in its edge zone is observed by magneto-optics. When the flux front reaches the inner boundary of the irradiated zone, magnetic flux leaks to the center and then gradually fills the unirradiated zone from the middle. We observe vortex motion against the flux-density gradient (driven by the vortex curvature) and large "overcritical" Meissner currents in the flux-free zone. The measured flux profiles agree with planar calculations assuming a nonlinear resistivity with different critical current densities in the central and edge zones of a disk or strip.

PACS numbers: 74.60.Ec, 74.60.Jg

One of the crucial properties of type-II superconductors is their nonlinear current-voltage curve caused by the interaction of Abrikosov flux lines with pinning centers in the matrix. The knowledge of the pinning and depinning mechanisms is particularly important for high temperature superconductors (HTSC's) in order to improve their performance in technical applications. In HTSC's the calculation of the critical current density j_c, above which a measurable voltage drop occurs, is complicated by the layered structure of these oxides, which causes pronounced material anisotropy and reduces the line tension of the flux lines to the point where they dissolve into nearly independent two-dimensional "pancake vortices" in the superconducting Cu-O layers [1]. This large anisotropy, the short coherence length ξ (which reduces the pinning energy), and the long magnetic penetration depth λ (which softens the flux-line lattice) lead to depinning by thermal activation, in particular at the high temperatures $T \approx 77$ K aimed at for applications.

While the detailed microscopic and statistical theory of the vortex-pin system is highly complicated [2], and new general pictures like vortex lattice melting [3], vortex glass scaling [4], and a Bose glass state [5] are conceptually difficult, from a phenomenological point of view the pinning problem is quite simple: For a wide class of experiments the low-frequency bulk magnetic response is characterized completely by the nonlinear resistivity $\rho(j) = E(j)/j$ of the superconductor. In particular, for a given geometry, in the approximation $H_{c1} = 0$ the field and current distributions in response to a varying applied field $H_a(t)$ are uniquely determined by the current-voltage law $E(j)$, which in general may depend on the flux density B and temperature T and on the orientations of B and j as parameters. This sometimes overlooked simplicity has recently been used in a comprehensive theoretical study [6] of flux creep in HTSC's in parallel magnetic field. In this *longitudinal* geometry, $\mathbf{B}(\mathbf{r},t)$, $\mathbf{j}(\mathbf{r},t) = (\partial H/\partial B)\nabla \times \mathbf{B}$, and $\mathbf{E}(\mathbf{r},t) = (\mathbf{j}/j)E(j)$ follow from the nonlinear diffusion equation $\partial \mathbf{E}/\partial t = D(E)\nabla^2 E$ with $D(E) = \mu_0^{-1}\partial E/\partial j$.

In the present paper we show that this simplicity holds also in the more realistic *perpendicular* geometry when a thin superconductor is placed into a time-dependent transverse magnetic field, in which its magnetic response is much larger than in a longitudinal field. We find that the space- and time-resolved penetration and exit of magnetic flux in HTSC platelets with inhomogeneous pinning introduced by high-energy heavy-ion irradiation of its edge zone, is well described by the planar approximation with a nonlinear sheet resistivity with spatially varying j_c.

Using a HTSC with a framelike zone of enhanced bulk pinning, we can simulate an edge barrier for flux penetration and study the large "overcritical" Meissner currents which flow in the weak-pinning central zone before flux has penetrated. Note that in *transverse* fields the observed surface barrier, which for weak pinning leads to a characteristic hysteresis, typically is *not* the microscopic Bean-Livingston barrier or barrier for penetration of pancake vortices [7], but rather a *macroscopic barrier* [8] that is due to the constant thickness (ellipsoids do not exhibit such a barrier) and is similar to the barrier observed in type-I superconductors with rectangular cross section [9]. For this natural geometric barrier, a finite lower critical field H_{c1} is crucial, while the artificial edge barrier of our specimens is caused by bulk pinning.

In perpendicular geometry, the magnetic field outside a thin conductor of thickness d is determined by its sheet current $\mathbf{J}(y,z) = \int_{-d/2}^{d/2} \mathbf{j}(x,y,z)\,dx$. For a circular disk with radius $a \gg d$ in a homogeneous field $H_a(t)$ along x one has $\mathbf{J} = \hat{\phi} J(r,t)$ where $r = (y^2 + z^2)^{1/2}$. In planar approximation the local field at the disk surfaces has the

0031-9007/94/73(10)/1424(4)$06.00
© 1994 The American Physical Society

components $H_r(r,t) = \pm\frac{1}{2}J(r,t)$ and [10,11]

$$H_x(r,t) = H_a(t) + \frac{1}{2\pi}\int_0^a P(r,u)J(u,t)\,du,$$

$$P(r,u) = \frac{E(k)}{r-u} - \frac{K(k)}{r+u}, k = \frac{(4ru)^{1/2}}{r+u}. \quad (1)$$

$E(k)$ and $K(k)$ are complete elliptic integrals. From (1) and the induction law $\mathbf{B} = \partial\mathbf{B}/\partial t = -\nabla\times\mathbf{E}$ with $\mathbf{B} \approx \mu_0\mathbf{H}$ (or $H_{c1} = 0$) one obtains an integral equation for the sheet current $J(r,t)$ [11],

$$J(r,t) = \tau(J)\left[\pi r\dot{H}_a(t) + \int_0^1 Q(r,u)\dot{J}(u,t)\,du\right],$$

$$Q(r,u) = \frac{1}{r}\int_0^r P(r',u)r'\,dr', \qquad \tau(J) = \frac{ad\mu_0}{2\pi\rho(J)}. \quad (2)$$

In (2) the disk radius a is chosen as unit length such that the prefactor τ becomes a relaxation time. For long strips, equations similar to (1) and (2) apply [11].

To simulate experiments we insert in (2) a model resistivity, say $\rho = (J/J_c)^n\rho_0$ ($n \gg 1$) with a critical sheet current $J_c(r,B) = j_c d$ which in general depends on the position r and perpendicular induction B. In regions with $B = 0$ we formally put $J_c = \infty$ or $\rho = 0$; this nontrivial assumption turns out to describe our experiments. Note that J causes parallel surface fields $H_r = \pm J/2$ which can generate longitudinal vortices at positions where $B = 0$. Apparently these parallel vortices are strongly pinned and do not limit the sheet current.

We integrate Eq. (2) on a personal computer by the method described in Ref. [11]. After tabulation of the kernels $P(r,u)$ and $Q(r,u)$, which are functions of one variable r/u, one discretizes the integrals using a grid with nonequidistant points $y_i = y(x_i)$ with, e.g., $x_i = (i - \frac{1}{2})/N$, $i = 1,...,N$, $y(x) = 3x^2 - 2x^3$ yielding a weight function $y'(x) = 6x(1-x)$ which vanishes at the integration boundaries. The resulting matrix $Q(r_i,u_j) = Q_{ij}$ is then inverted to solve Eq. (2) for $\dot{J} = \partial J/\partial t$. This inversion allows direct time integration of (2) by a Runge-Kutta method for given applied field $H_a(t)$, starting, e.g., with $J(r,t=0) = 0$ if $H_a(t=0) = 0$. Various nonlinear problems may be solved in this way:

(a) Quasistatic penetration of flux is simulated by increasing $H_a(t)$ slowly with constant ramp rate $\dot{H}_a$.

(b) Periodic penetration and exit of flux is simulated by cycling $H_a(t)$, e.g., zig-zag-like with amplitude H_0, period $2t_0$, and ramp rate $\dot{H}_a(t) = (H_0/t_0)\,\mathrm{sgn}[\cos(\pi t/t_0)] = \pm H_0/t_0$. Such cycling describes our experiment and also yields hysteresis loops of the magnetization curve $M(H_a)$ where $M = \pi\int_0^a J(r)r^2\,dr$ is the magnetic moment of the disk. The analytic solutions for the disk [12] and strip [13] with $J_c = \mathrm{const}$ are reproduced in this way.

(c) Flux creep in perpendicular geometry [14] is simulated after the increase of $H_a(t)$ is stopped.

In this Letter we concentrate on quasistatic flux penetration; field cycling and creep will be discussed elsewhere. We compare our magneto-optic observations with computations for a disk with radius $a = 1$ and long strip with half width $a = 1$ (coordinate y); both geometries yield very similar current and field profiles. We simulate inhomogeneous pinning by choosing critical sheet currents $J_{c1} = 1$ for $r > r_1$ ($|y| > r_1$) and $J_{c2} = 0.05$ for $r \le r_1$ ($|y| \le r_1$) with $r_1 = 0.72a$. Thus, J_{c1} and a are our field and length units. At positions where $|H| < 0.01$ we put $J_c \gg 1$. This space- and field-dependent J_c enters our current-voltage curve $E(J) = 0.2(J/J_c)^{19}$. Our ramp rate is $\dot{H}_a = 0.01$, thus $H_a(t) = 0.01t$.

The result for a strip in increasing field is shown in Fig. 1. For $t \le 23$, corresponding to $H_a \le 0.23 \approx (J_{c1}/\pi)\mathrm{arccosh}(a/r_1)$ [13], we obtain the analytical profiles $H(y,t)$ of Ref. [13], which exhibit $H = 0$ and a Meissner current $J \le J_{c1}$ in the flux-free region $|y| < b$, and $J = J_{c1}$ in the penetrated region $|y| > b$, since the flux front is still at $b \ge r_1$. At $t = 23$ ($H_a = 0.23$) the flux front [or its foot caused by our smooth $E(J)$] has reached the weak-pinning zone $|y| < r_1$. With further

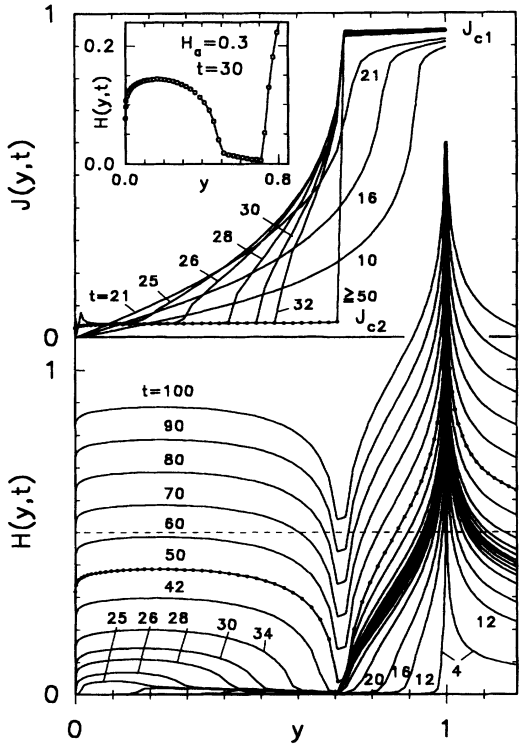

FIG. 1. Calculated profiles of the sheet current $J(y,t)$ (top) and perpendicular magnetic field $H(y,t)$ (bottom) for a thin superconducting strip of width 2 extending from $y = -1$ to $y = 1$ in an applied magnetic field which increases as $H_a(t) = 0.01t$. Parameter is the time $t = 4$, 12, 16, 20, 22, 23, 24, 25, 26, 28, 30, 40, 50, and > 50. Pinning is enhanced in the zone $0.72 \le |y| \le 1$. The inset shows the enlarged field profile at $H_a = 0.3$. The dots indicate the grid. The dashed line denotes the applied field $H_a = 0.5$ at which flux filling of the weak-pining zone $|y| < 0.72$ is complete (dotted profiles).

increase of H_a, magnetic flux starts to leak into the specimen center where it piles up such that in the zone between this central flux heap and r_1 one still has nearly zero field $|H| < 0.01$ (see inset in Fig. 1) and large overcritical Meissner current $J > J_{c2}$. Inside the central flux heap, J is suppressed to the small critical value $J_{c2} = 0.05$, except near the very center where $|H| < 0.01$ allows for a cusp of J. [Actually, this means two closely spaced cusps of opposite sign since $J(-y) = -J(y)$, and a narrow dip in H since $H(-y) = H(y)$.] The central flux heap grows both in extension and height until the weak-pinning zone is completely filled at $t = 50$ ($H_a = 0.5$).

Remarkably, until this filling is completed one has $H(r_1) = 0$ for all times $t \leq 50$. This unexpected finding of zero field at the irradiation boundary is seen in all our simulations and is in agreement with our experiments. After $t = 50$, the sheet current stays piecewise constant, $J(|y| < r_1) \approx 0.05$ and $J(|y| > r_1) \approx 1$. Consequently, the magnetic moment also saturates, the electric field becomes linear, $E = -\mu_0 \dot{H}_a y = -0.01y$, and the magnetic field profile moves up such that its shape $H(y,t) - H_a(t)$ stays unchanged. The logarithmic infinity of the theoretical field profile at the specimen edge $r = a$ or $|y| = a$ is due to our assumption $d \ll a$.

Our single crystals of $Bi_2Sr_2CaCu_2O_{8+\delta}$ (Bi2212) were irradiated with 860 MeV Xe ions at GANIL (Caen, France) in order to produce enhanced pinning at the edges. This high-energy heavy ion irradiation produces columnar defects which prove to be very effective pinning sites in HTSC [15] and increase the critical current density by factors of at least 20 to 50 depending on temperature and fluence; at $T = 50$ K the unirradiated sample possibly was even above the depinning line. During the irradiation, the center of the sample was covered by an absorber to expose only the outer regions of the sample to the ion beam, Fig. 2(a). Later the absorber was removed by an organic solvent. The Bi2212 single crystals were prepared as described in Ref. [16].

To visualize the magnetic flux distribution we use the magneto-optical Faraday effect in ferrimagnetic garnet films with an in-plane anisotropy. The full description of this technique is given in Ref. [17]. The obtained results are illustrated on a sample which was irradiated with a fluence $\phi t = 5 \times 10^{10}$ ions/cm^2.

Figure 2(a) shows the shape of the Bi2212 single crystal and the location of the absorber, the bright area in the sample center. In the sequence of Figs. 2(b)–2(f) flux distributions are presented at temperature $T = 50$ K for applied transverse fields of $\mu_0 H_a = 85$ mT (b), 107 mT (c), 128 mT (d), 150 mT (e), and 171 mT (f). The brighter contrast on the photographs corresponds to higher local magnetic field H_x; the darkest areas show the Meissner phase where $H_x = 0$. The black lines indicate the sample edge. Figure 2(b) shows that the vortices penetrate into the superconductor only from the edges, mainly in the middle of each edge since screening currents and stray field are maximum there [18]. In Fig. 2(c) the flux front

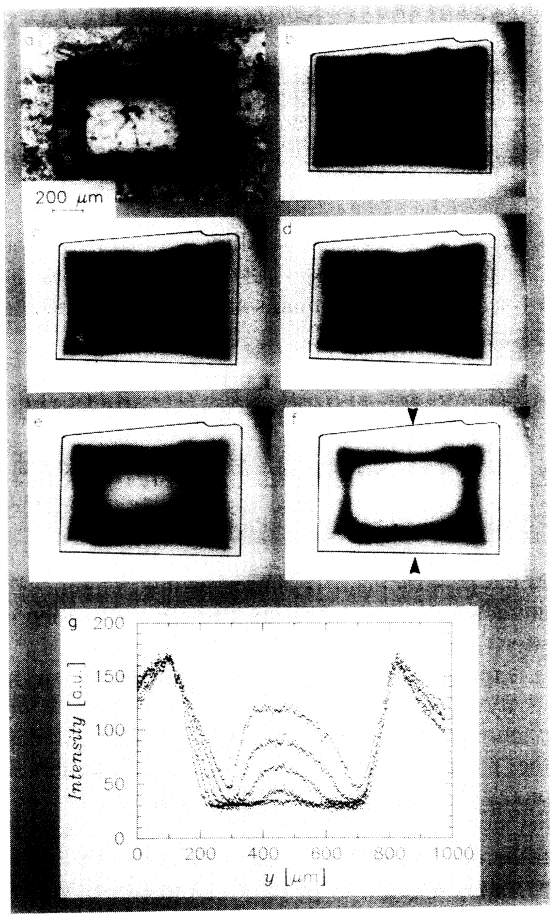

FIG. 2. (a) Shape of the irradiated Bi2212 single crystal. The absorber is visible as bright region in the sample center. (b) Flux distribution at $T = 50$ K in a transverse magnetic field of $\mu_0 H_a = 85$ mT. (c) $\mu_0 H_a = 107$ mT. The flux starts to penetrate the unirradiated part of the sample at the narrowest place of the irradiated belt (white arrow in the lower left corner) and piles up in the sample center as indicated by the other white arrow. (d) $\mu_0 H_a = 128$ mT. (e) $\mu_0 H_a = 150$ mT. (f) $\mu_0 H_a = 171$ mT. (g) Flux density profiles taken from (b)–(f) along the line indicated by two arrows in (f). The measured field profiles nicely agree with the calculated ones shown in Fig. 1.

reaches the unirradiated area at the narrowest place of the irradiated belt [white arrow in the lower left corner in Fig. 2(c), see also Fig. 2(a)].

Now an interesting phenomenon occurs: Flux suddenly appears in the center of the Meissner area (white arrow in the sample center). At the same time, the motion of the flux front from the sample edges slows down and the magnetization is dominated by the spread of flux from the center. Since vortices cannot nucleate at the sample center, they have to cross the Meissner area being driven to the center by screening currents which are much higher ("overcritical") than the j_c in this unirradiated region, Figs. 2(e)–2(f). This situation is analogous to the penetration of flux bundles over an edge barrier observed in type-I superconductors [19]. The central flux pileup

and the geometric surface barrier both would be absent in pin-free ellipsoids (which exhibit constant B), but they occur when near the edges the specimen is either *thicker* than an ellipsoid with same axes [8] and/or has *enhanced edge pinning* like our samples; both measures enhance the screening current near the edges. The central flux pileup in similar samples was observed recently also with Hall-probe arrays by Zeldov *et al.* [20].

The appearance and growth of the magnetic flux in the sample center is clearly seen in the flux-density profiles measured across the sample, Fig. 2(g). These profiles nicely agree with the calculated field profiles of Fig. 1. Moreover, the "uphill motion" of flux lines, predicted in Ref. [13], is clearly seen: During the growth of the central flux heap the arriving flux lines move against the flux-density gradient since the driving current in this geometry is caused by the *curvature* of the flux lines. Notice that the measured profiles do not show a sharp cusp at the sample edge since the garnet film saturates at a magnetic field of about 200 mT.

The agreement between our simple theory and the experiment is not trivial. First, it shows that a planar theory which considers only the averaged components of j and E parallel to a specimen of finite thickness is sufficient. Second, this agreement also means that in the unirradiated zone pinning is weak only for *perpendicular* flux, but it is strong enough to prevent *parallel* flux lines to penetrate from the flat surfaces, probably due to intrinsic pinning by the Cu-O layers. Notice that the large Meissner screening current J, or its parallel surface field $\pm J/2$, generates parallel vortices of opposite orientation, which without this pinning would penetrate and annihilate such that the magnetic field lines *close around the irradiated frame* as in a current carrying loop. This would cause a negative cusp of H_x at the inner edge of the irradiated zone, which is not observed in our experiments, thus confirming our assumption $J_c(B = 0) = \infty$.

In summary, by magneto-optics we observed flux penetration into a Bi2212 platelet with irradiation-enhanced bulk pinning near its edge. The obtained flux-density profiles in increasing applied field $H_a(t)$ agree with those calculated by assuming $H_{c1} = 0$ and a nonlinear current-voltage law with two different critical current densities in the irradiated and unirradiated zones, and "unlimited" current density at positions where $B = 0$. The importance of the latter assumption in the presence of inhomogeneous pinning is illustrated here for the first time. Nice agreement between theory and experiment is also found when $H_a(t)$ is cycled and when the hysteretic magnetic moment is measured. This will be the subject of a forthcoming paper [21].

After this work was completed we received a preprint [20] which presents exact analytical solutions to the quasistatic flux penetration into superconducting strips of constant thickness, which agree well with our experiments and computations.

We thank T. W. Li and the Dutch FOM (ALMOS) for the crystals.

*Institute of Solid State Physics, Russian Academy of Science, 142432 Chernogolovka, Russia.

[1] J. R. Clem, Phys. Rev. B **43**, 7837 (1991); D. Feinberg, Physica (Amsterdam) **194C**, 126 (1992).
[2] G. Blatter *et al.*, Rev. Mod. Phys. (to be published).
[3] D. R. Nelson and H. S. Seung, Phys. Rev. B **39**, 9174 (1989).
[4] D. S. Fisher, M. P. A. Fisher, and D. A. Huse, Phys. Rev. B **43**, 130 (1991).
[5] D. R. Nelson and V. M. Vinokur, Phys. Rev. Lett. **68**, 2389 (1993); Phys. Rev. B **48**, 13 060 (1993).
[6] A. Gurevich and H. Küpfer, Phys. Rev. B **48**, 6477 (1993).
[7] L. Burlachkov, Phys. Rev. B **47**, 8056 (1993); A. Buzdin and D. Feinberg, Phys. Lett. A **165**, 281 (1992); R. G. Mints and I. B. Snapiro, Europhys. Lett. **21**, 611 (1993); Phys. Rev. B **47**, 3273 (1993).
[8] M. V. Indenbom, H. Kronmüller, T. W. Li, P. H. Kes, and A. A. Menovsky, Physica (Amsterdam) **222C**, 203 (1994); M. V. Indenbom and E. H. Brandt (unpublished).
[9] J. Provost, E. Paumier, and A. Fortini, J. Phys. F **4**, 439 (1974).
[10] D. J. Frankel, J. Appl. Phys. **50**, 5402 (1979); M. Däumling and D. C. Larbalestier, Phys. Rev. B **40**, 9350 (1989); L. W. Conner and A. P. Malozemoff, Phys. Rev. B **43**, 402 (1991); H. Theuss, A. Forkl, and H. Kronmüller, Physica (Amsterdam) **190C**, 345 (1992).
[11] E. H. Brandt, Phys. Rev. Lett. **71**, 2821 (1993); Phys. Rev. B **49**, 9024 (1994).
[12] P. N. Mikheenko and Yu. E. Kuzovlev, Physica (Amsterdam) **204C**, 229 (1993).
[13] E. H. Brandt, M. Indenbom, and A. Forkl, Europhys. Lett. **22**, 735 (1993); E. H. Brandt and M. Indenbom, Phys. Rev. B **48**, 12 893 (1993); E. Zeldov *et al.*, Phys. Rev. B **49**, 9802 (1994).
[14] A. Gurevich and E. H. Brandt, Phys. Rev. Lett. **73**, 178 (1994).
[15] L. Civale *et al.*, Phys. Rev. Lett. **67**, 648 (1991); M. Konczykowski *et al.*, Phys. Rev. B **44**, 7167 (1991); W. Gerhäuser *et al.*, Phys. Rev. Lett. **68**, 879 (1992); V. Hardy *et al.*, Physica (Amsterdam) **201C**, 85 (1992); M. Leghissa *et al.*, Europhys. Lett. **11**, 323 (1992); Th. Schuster *et al.*, Phys. Rev. B **46**, 8496 (1992); Th. Schuster *et al.*, Physica (Amsterdam) **203C**, 203 (1992).
[16] T. W. Li *et al.*, J. Cryst. Growth **135**, 481 (1994).
[17] L. A. Dorosinskii, M. V. Indenbom, V. I. Nikitenko, Yu. A. Ossip'yan, A. A. Polyanskii, and V. K. Vlasko-Vlasov, Physica (Amsterdam) **203C**, 149 (1992).
[18] Th. Schuster, M. V. Indenbom, M. R. Koblischka, and H. Kuhn, H. Kronmüller, Phys. Rev. B **49**, 3443 (1994).
[19] R. P. Huebener, R. T. Kampwirth, and J. R. Clem, J. Low Temp. Phys. **6**, 275 (1972).
[20] E. Zeldov *et al.*, following Letter, Phys. Rev. Lett. **73**, 1428 (1994).
[21] Th. Schuster, H. Kuhn, E. H. Brandt, M. V. Indenbom, M. R. Koblischka, and M. Konczykowski (unpublished).

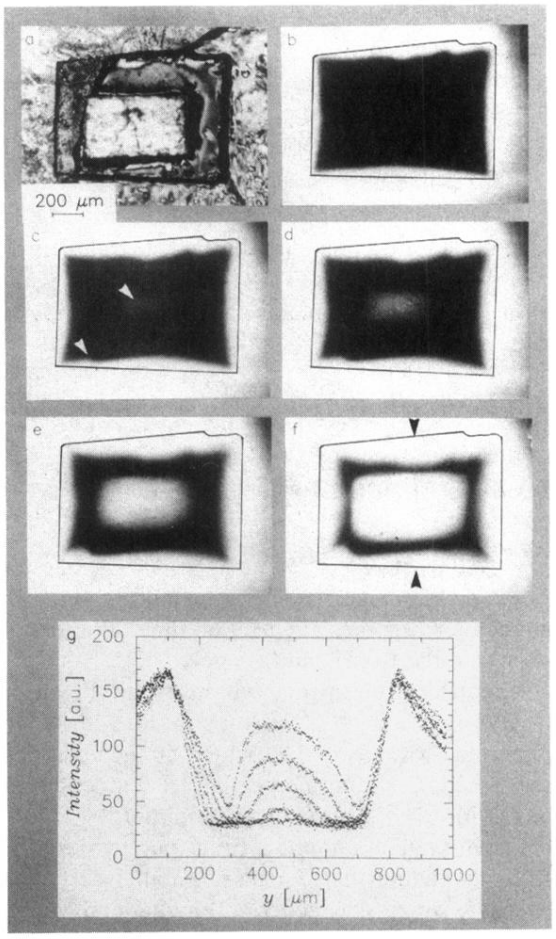

FIG. 2. (a) Shape of the irradiated Bi2212 single crystal. The absorber is visible as bright region in the sample center. (b) Flux distribution at $T = 50$ K in a transverse magnetic field of $\mu_0 H_a = 85$ mT. (c) $\mu_0 H_a = 107$ mT. The flux starts to penetrate the unirradiated part of the sample at the narrowest place of the irradiated belt (white arrow in the lower left corner) and piles up in the sample center as indicated by the other white arrow. (d) $\mu_0 H_a = 128$ mT. (e) $\mu_0 H_a = 150$ mT. (f) $\mu_0 H_a = 171$ mT. (g) Flux density profiles taken from (b)–(f) along the line indicated by two arrows in (f). The measured field profiles nicely agree with the calculated ones shown in Fig. 1.